XI National and II International Engineering Thermodynamics Congress

Paper Number: 29147

Methodology for the calculation of the shadow factor on roofs and facades of buildings in urban areas

Joan D. Viana-Fons*, José Gonzálvez-Maciá, Jorge Payá

Instituto Universitario de Investigación de Ingeniería Energética (IUIIE), Universitat Politècnica de València, Camino de Vera s/n, Ed 8E, Semisótano frente Acceso J, 46022 València, Spain.

*Corresponding author. E-mail address: jviana@iie.upv.es

ABSTRACT

The present paper presents a systematic methodology to obtain the shadow factor on roofs and facades of buildings. The approach is based on the use of Geographic Information Systems (GIS), and helps to obtain, accurately and on urban scale, the incident solar irradiance on each surface of any building. Given the characteristics of the entire urban area, the solar gain of the buildings can consequently be calculated more accurately than with a stand-alone building model. A good quantification of the solar gain is essential, for instance, to better evaluate the consumption of Air-Conditioning systems. This approach can also be useful to size and simulate the introduction of PV panels in facades or roofs of urban regions, or to carry out a climate-sensitive urban design and planning.
This approach is based on a vector-based 3D model of the buildings or trees of the urban region. Open data of cadastral cartography and LiDAR altimetric data are used as inputs. Using the previous 3D model and solar geometry data, analytical models are applied to calculate the shadow of each tree or building on any desired surface.
The mentioned methodology has been implemented in R and has been applied to buildings of Valencia (Spain). The results have been validated with SketchUp, both for horizontal and vertical surfaces, and the error has been calculated for different hours of the day.

Keywords: *Solar energy, GIS-based approach, Shadow factor, LiDAR*

1. Introduction

The building sector is responsible for almost a third of the final energy consumption in the world [1], thus it represents a considerable energy-saving potential and plays an important role in addressing climate change. In urban areas, there is a strong relationship between municipal planning, the promotion of energy efficiency and the use of renewable energies. As such, a proper solar resource assessment (SRA) can help to reduce the energy demand while shifting towards on-site renewable energy generation by the use of passive and active solar energy systems. Likewise, SRA enables to evaluate and simulate the solar heat gain and daylight resulting from urban geometry and helping in the analysis, design and optimization of the building thermal and daylighting systems.

The use of Geographic Information Systems (GIS) and remote sensing, as LiDAR, enable to develop and implement useful tools capable to obtain the solar resource of sufficient accuracy and spatial extension required in complex sites such as urban environments [2]. In this context, the incident solar irradiance and daylight are strongly influenced by the built environment and density of the urban space, especially in metropolitan downtown areas, where the landscape does present large discontinuities that cast intricate shadow outlines. In these conditions, shading analysis becomes essential to perform suitable solar resource maps. Thus, many methods have been proposed to estimate the solar resource

using remote sensing data in an urban environments [3, 4]. Such methods are usually performed employing raster-based models [5–8], operated on a Digital Elevation Model (DEM), and applying the available software for raster-based shadow calculations, such as r.sun model [9] in GRASS GIS or the Solar Analyst extension in ArcGIS. However, the raster-based models are not appropriate for modelling vertical surfaces, intrinsic to urban areas, since they are represented as discontinuities and cannot be evaluated. In this context, vector-based models are more appropriate to model and analyze urban spaces and recent publications contribute to advancing in this direction [10, 11].

This paper presents a systematic methodology, which integrates two detailed models, that enables to obtain, accurately and on urban scale, a vector-based 3D model of the buildings and trees upon which the incident solar irradiance on both horizontal and vertical surfaces are calculated, taking into account the shading conditions for the direct and the diffuse components. The assessed area are buildings of the Faculty of Computer Science and its surroundings at Universitat Politècnica de València in the east of Spain (Figure 1).

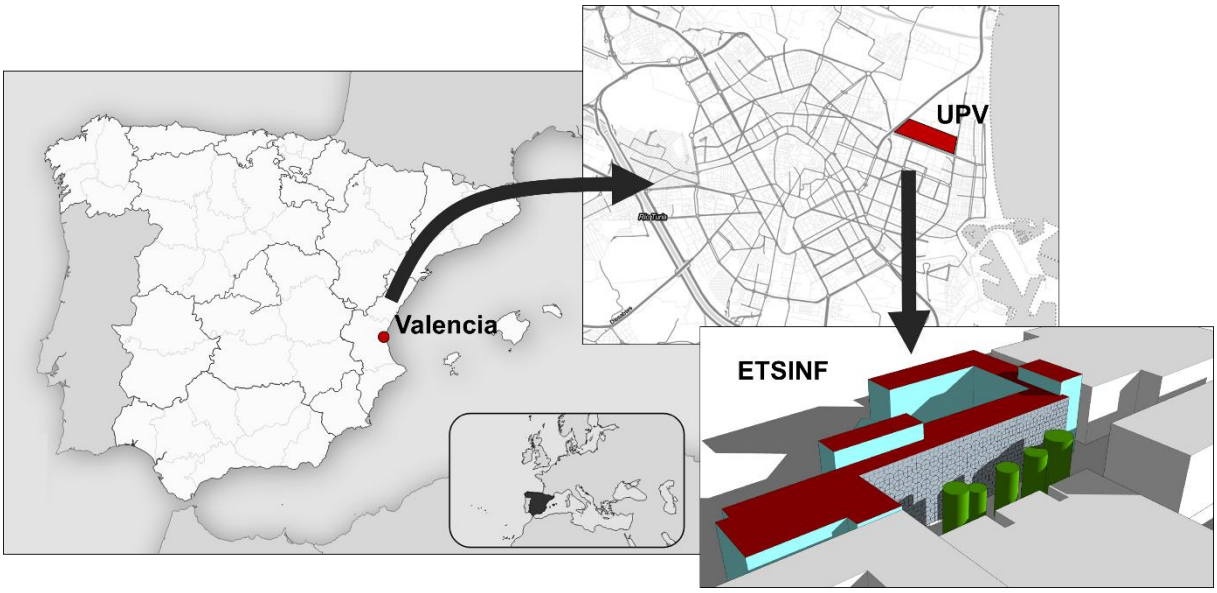

Figure 1. Location of the case study site in Valencia, Spain

2. Methodology

The proposed methodology consists in the integration of two coupled models (Figure 2) that, starting from geographical data, help to obtain the 3D model, including buildings and trees, of the studied urban area. Based on this model, a 3D grid of the studied surfaces, roofs and facades, is performed. Then, the Shading Factor (SF) and the Sky View Factor (SVF) of each grid point are obtained considering the modelled surrounding elements and the sun's position at the given location. Finally, based on the available beam and diffuse horizontal irradiance, extracted from the Typical Meteorological Year (TMY) of the studied area, the hourly time series of the total irradiance are calculated for each grid point.

On the one hand, a GIS-based model has been developed in order to obtain a set of polygons representing the buildings and the trees of the studied area. As a result, a prismatic model of the city has been obtained, which comply to the block model (LOD1) according to the level of detail categorization defined by the standard CityGML [12]. The selection of this type of approach is consistent with Wang et al. [13], which states that the prismatic modeling is suitable for multilevel flat buildings, which prevailing in urban areas in Spain.

The model of the buildings is obtained starting from their footprints and the related LiDAR (Light Detection and Ranging) point clouds. Once the altimetric information of each individual polygon are

isolated, the height of each surface is modelled as the median of the Z values contained in each polygon. Finally, the height obtained of each polygon is validated using its CAD elevation view.

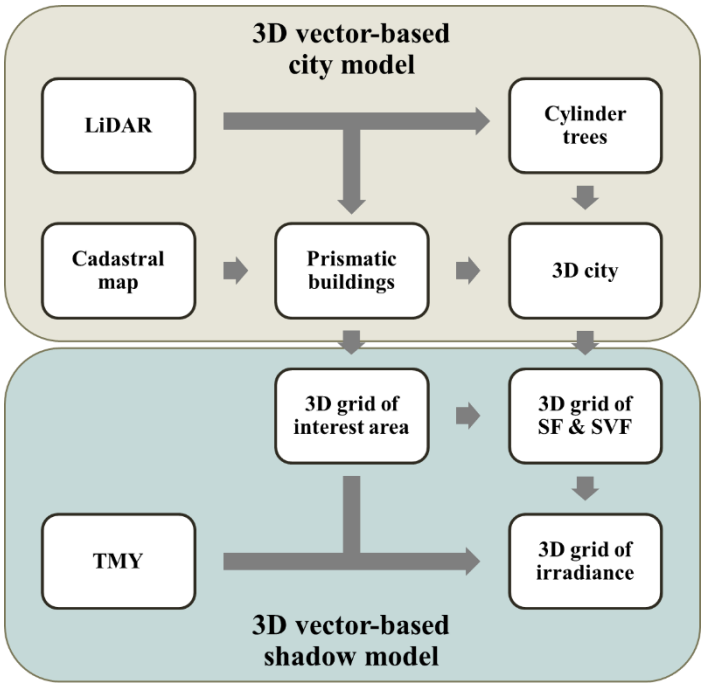

Figure 2. Workflow of the proposed methodology

The trees are modelled as cylinders, characterized by the treetop XY coordinates, the crown radius and the height. First, based on the LiDAR point clouds, a point-to-raster approach is applied obtaining the canopy height model (CHM) of the studied area. Then, the variable window filter (VWF) algorithm developed by Popescu and Wynne [14] is employed for detecting the treetops, based on a window's size function which relates the height and the crown radius of the tree. Once the XY coordinates of the treetops are found, the cylinders representing the trees are generated using the height, extracted from the CHM, and the crown radius, obtained through the VWF algorithm. The results of this model are validated using the 3D model of Google Earth to check the position, height and crown's area of the modelled trees.

On the another hand, the shadow algorithm developed by Vulkan et al. [15] is applied in order to obtain the shading conditions of studied surfaces. Based on the obtained vector-based 3D model of the city, a regular grid of the studied surfaces, both roofs and facades, are performed using a given resolution. Then, the Shading Factor – i.e. losses of the beam irradiance component – and the Sky View Factor – i.e. losses of the diffuse irradiance component – is calculated in each point of the grid using geometric models.

The Shading Factor of a grid point at any given time is the result of the evaluating if this 3D point is in shadow or not. Then, it can be calculated using trigonometric relations based on the sun's position – i.e. elevation and azimuth – and the obstacles along the sunray. In order to calculate the SF along the year of a given point, the method employed starts from the 3D polygons of the surroundings and it is applied to the hourly time series of the sun's position using the algorithms provided by the NOAA [16].

The Sky View factor is the viewed proportion of the sky hemisphere at a given point. It is independent of the sun's position and only depends on the surroundings' geometry. It is calculated using a given angular resolution of the azimuthal plane and applying for each view direction the geometrical model proposed by Gál and Unger [17].

Finally, the hourly time series of the total solar irradiance G is calculated for each grid point using the horizontal direct B_0 and diffuse D_0 component values of the Typical Meteorological Year (TMY) obtained from the web service provided by the JRC [18]. Then, based on the surface orientation, the hourly shading conditions and solar radiation along the TMY, the annual total solar insolation I_G for each grid point is calculated using the following equation:

$$I_G = \sum_{t=1}^{8760} G(t) = \sum_{t=1}^{8760} SF(t) \cdot B_0(t) \cdot \frac{\cos(\theta(t))}{\sin(\alpha(t))} + SVF \cdot D_0(t) \quad (1)$$

Denoting θ as the solar incidence angle and α the solar elevation angle.

3. Results and discussion

The previous methodology has been applied to the building of the Faculty of Computer Science (ETSINF) and surroundings at the Universitat Politècnica de València (39°28′58″N, 0°20′52″O) in the east of Spain (Figure 1).

The building model was performed employing the cadastral map of the assessed area, available from http://www.sedecatastro.gob.es/, and the related low-resolution LiDAR point clouds (0.5 points/m^2), published by the Spain's National Geographic Institute [19]. As a result, a GIS-based model of the extruded polygons representing the buildings were obtained. The results were validated using the CAD elevation views of the construction drawings of the modelled surfaces (Figure 3). The results show that the model produces good height estimates, obtaining for the modelled surfaces a root mean square error (RMSE) of 0.53m and maximum relative error of 4.7%.

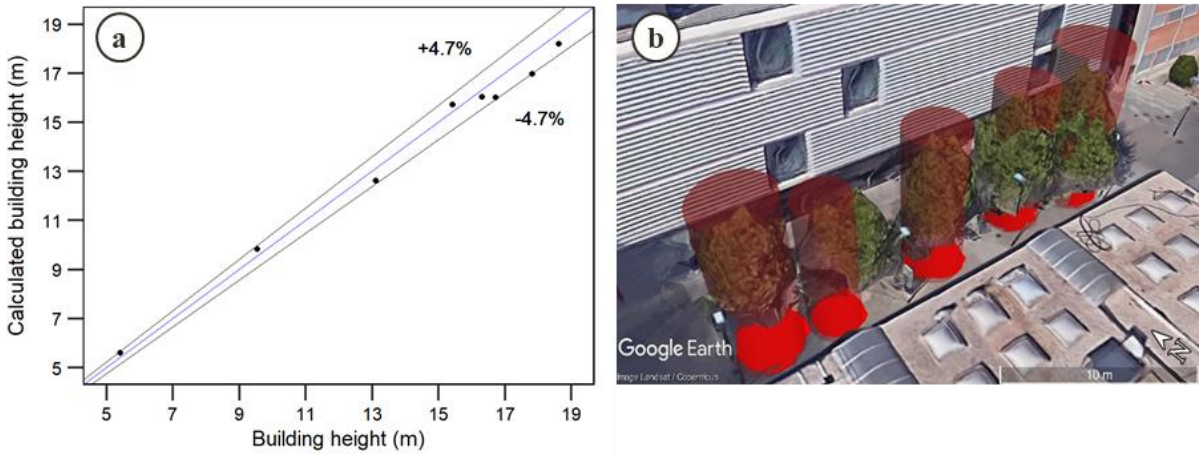

Figure 3. Results and validation of the 3D model. a) Validation of the height obtained by the prismatic building model compared with their CAD elevation viwes and b) Cylinder tree model results compared with the 3D model of Google Earth.

The tree model was performed employing the same LiDAR point cloud dataset than the building model. The CHM was obtained using a resolution of 2 meters, consistent with the LiDAR point density. Likewise, the variable window filter algorithm were applied using a linear function to define the size of the window on the canopy given the height of the pixel. As a result, the trees of the studied area were detected and characterized according to height and crown radius. Figure 3 shows the cylinders representing the trees obtained superimposed on the 3D model of Google Earth. The figure shows that the model produces good estimates of the treetop position, crown's area and height taking into account the low-resolution of the employed LiDAR dataset.

Once the vector-based model was obtained, a 3D grid of the studied surfaces was generated. The grid size was selected using the best compromise between accuracy and computational time according to Peronato et al. [20], who conclude that the error up to a 2-m grid size is negligible for solar radiation

studies. Likewise, the buildings and trees were modelled in Google SketchUp in order to validate the shading results in a 3D CAD environment.

The Shading Factor was obtained for each grid point along the year using the hourly time series of elevation and azimuth of the sun in the given location (Figure 4). The results were validated on December 21, both for facades and roofs of the building, using the SketchUp model of the studied area. Table 1 shows the success rate of the model, for each hour, compared with the shadow conditions obtained with SketchUp over the same grid points.

Table 1. Success rate of the Shading Factor model, for each hour on December 21, compared with the shadow conditions obtained with SketchUp over the same grid points. The fraction showed represents the number of correctly modelled grid points over the total grid points.

		Local time (h) on December 21									
		9:00	10:00	11:00	12:00	13:00	14:00	15:00	16:00	17:00	Mean
SF success rate	Facade	214/216	215/216	215/216	210/216	212/216	215/216	216/216	210/216	215/216	0.989
	Roof	220/227	223/227	226/227	221/227	225/227	227/227	226/227	225/227	226/227	0.988

Therefore, Shading Factor is calculated with high accuracy both for facade and roof surfaces, with a mean error of 1.1% and 1.2% respectively. Such low error values are due the geometric nature of the shadow cast model and the differences between the models can be explained by the errors in the 3D model and the solar position algorithms employed by each.

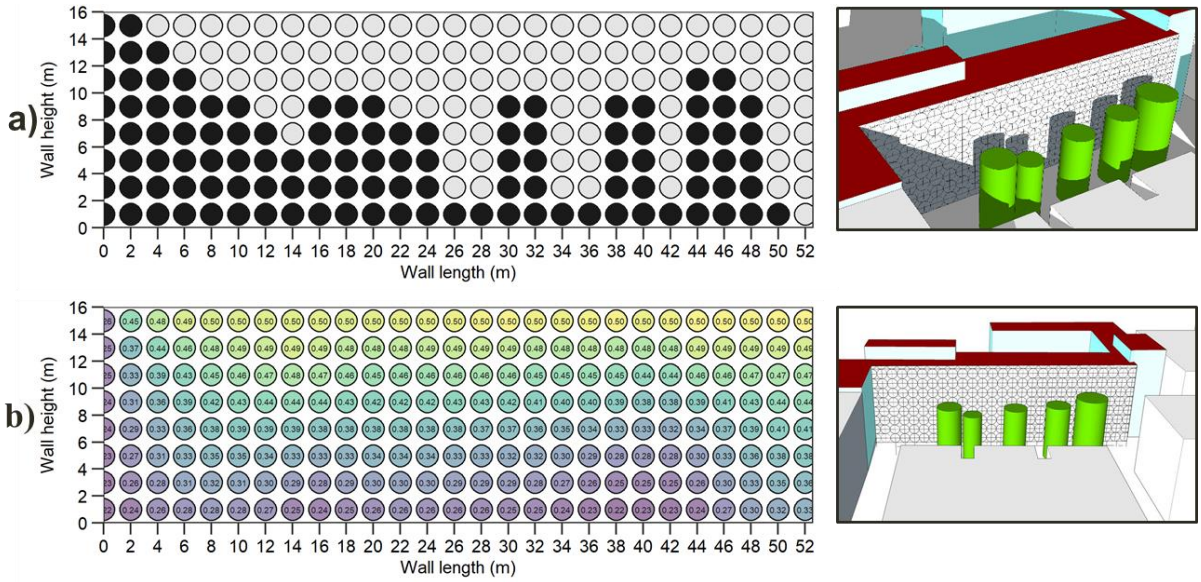

Figure 4. Results of shading effects on a facade. a) Shadow factor at 17:00 on December 21 and b) Sky View Factor

The Sky View Factor was obtained for each grid point using an azimuthal angular resolution of 5 degrees. Figure 4 gives the SVF obtained for a grid of an assessed wall. The results show that the values for the highest points of the wall are close to the maximum SVF of a vertical surface – i.e. there are not obstacles up to 15 meters – and it decreases with the wall height.

Finally, the hourly irradiance components were obtained for each grid point (Figure 5) by means of their surface orientation, their hourly shading conditions and the horizontal solar irradiance components along

the TMY. Table 2 summarizes the main results, both for facades and roofs, related with the annual insolation components and the shading effects.

Table 2. Radiation and shading results on the assessed building

	I_B/I_G (%)	I_D/I_G (%)	$I_B / I_{B\text{-}ns}$ (%)	$I_D / I_{D\text{-}ns}$ (%)	$I_G / I_{G\text{-}ns}$ (%)
Facades	66.14	33.86	54.89	74.57	62.40
Roofs	54.37	45.63	85.45	84.38	85.09
Total	60.26	39.74	68.29	78.54	72.00

$I_{G\text{-}ns}$,$I_{B\text{-}ns}$,$I_{D\text{-}ns}$: Annual total/direct/diffuse insolation without considering shading effects
I_G,I_B,I_D: Annual total/direct/diffuse insolation considering shading effects

On the one hand, the results show that two thirds of the total solar insolation stem from the direct component in roof surfaces, while its contribution is reduced to 54% in facades and 60% in all surfaces together. Furthermore, both components have a similar weight and the study of each of them is required to properly quantify the total incident radiation on both horizontal and vertical surfaces.

On the another hand, shading effects reduce 28% the incident total solar insolation on the building, decreasing 32% the direct component and 21% the diffuse component. Such high values are due the losses on facades, since the reduction on roofs is around 15% both in direct and diffuse components. Therefore, shading analysis is fundamental to correctly estimate the solar resource in buildings, since it has a significant impact on the incident insolation.

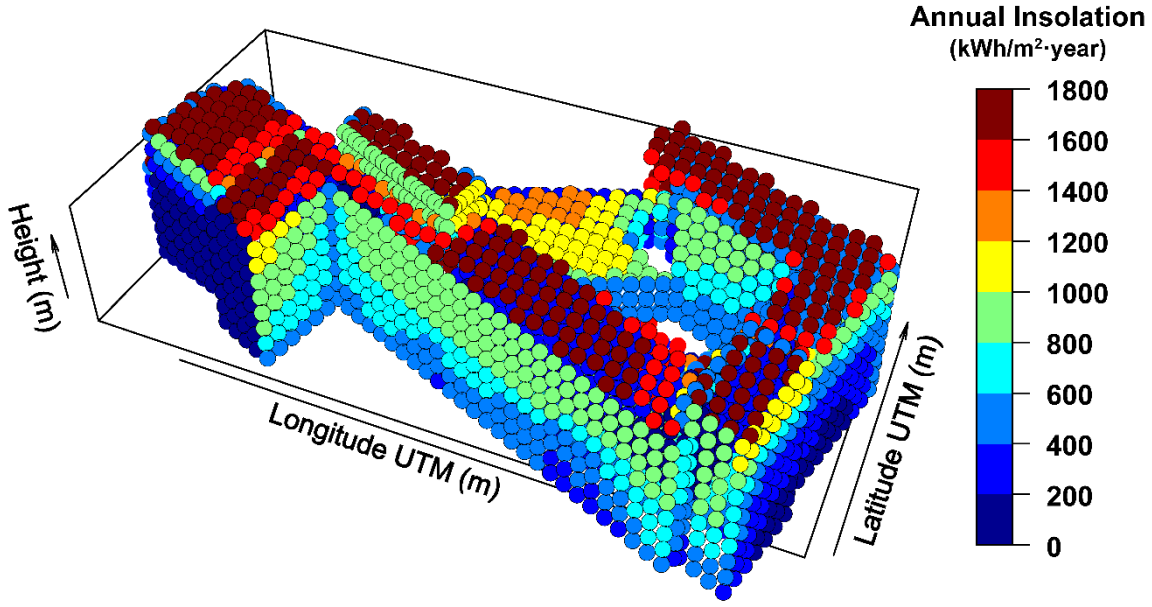

Figure 5. Total annual insolation for the assessed building

4. Conclusions

This document proposed a systematic methodology, applied from Geographic Information Systems (GIS) and implemented in R, which integrates two detailed models that enables to obtain, accurately and on urban scale, the 3D model of the existing buildings and trees upon which the shading conditions and the incident solar irradiance are calculated.

The developed vector-based model enables to obtain a 3D grid of the studied surfaces, both for roofs and facades, of an arbitrary spatial resolution. Likewise, the shading conditions and the incident solar irradiation can been obtained for each grid point in any temporal resolution.

The methodology has been applied to buildings of Valencia (Spain) and validated using Google SketchUp. The results showed that shading analysis is essential to properly estimate the solar resource on buildings, since it can significantly reduce the incident total solar insolation on their surfaces, especially on facades. Likewise, the results indicate that the quantification of both the solar irradiance components, direct and diffuse, is required to suitably evaluate the total incident insolation, on both horizontal and vertical surfaces, since they have a similar weight in the studied area.

The proposed approach is applicable to most regions, where LiDAR and long-term meteorological data is available, in order to carry out solar resource assessments at building, neighborhood or city scale.

5. Acknowledgements

The authors gratefully acknowledge José Fabuel Darocha from the Universitat Politècnica de València for providing the building maps that have helped to validate the models.

REFERENCES

[1] IEA. *Buildings - Tracking Clean Energy Progress*. 2019 [accessed. 2019-01-07]. Available at: https://www.iea.org/tcep/buildings/

[2] DAWOOD, N; DAWOOD, H; RODRIGUEZ-TREJO, S; CRILLY, M. *Visualising urban energy use: the use of LiDAR and remote sensing data in urban energy planning*. *Visualization in Engineering*. 2017, **5**(1), 22.

[3] FREITAS, S; CATITA, C; REDWEIK, P; BRITO, M C. *Modelling solar potential in the urban environment: State-of-the-art review*. *Renewable and Sustainable Energy Reviews*. 2015, **41**, 915–931.

[4] M. MARTÍN, A; DOMÍNGUEZ, J; AMADOR, J. *Applying LIDAR datasets and GIS based model to evaluate solar potential over roofs: a review*. *AIMS Energy*. 2015, **3**(3), 326–343.

[5] OH, M; PARK, H-D. *A new algorithm using a pyramid dataset for calculating shadowing in solar potential mapping* . *Renewable Energy* . 2018, **126**, 465–474.

[6] SUOMALAINEN, K; WANG, V; SHARP, B. *Rooftop solar potential based on LiDAR data: Bottom-up assessment at neighbourhood level*. *Renewable Energy*. 2017, **111**, 463–475.

[7] CATITA, C; REDWEIK, P; PEREIRA, J; BRITO, M C. *Extending solar potential analysis in buildings to vertical facades*. *Computers and Geosciences*. 2014, **66**, 1–12.

[8] REDWEIK, P; CATITA, C; BRITO, M. *Solar energy potential on roofs and facades in an urban landscape*. *Solar Energy*. 2013, **97**, 332–341.

[9] HOFIERKA, J; SÚRI, M. *The solar radiation model for Open source GIS: implementation and applications*. In: *Open source GIS - GRASS users conference*. 2002.

[10] LIANG, J; GONG, J; ZHOU, J; IBRAHIM, A N; LI, M. *An open-source 3D solar radiation model integrated with a 3D Geographic Information System*. *Environmental Modelling & Software*. 2015, **64**, 94–101.

[11] DORMAN, M; VULKAN, A; ERELL, E; KLOOG, I. *shadow : R Package for Geometric Shadow Calculations in an Urban Environment*. 2017, 1–21.

[12] GRÖGER, G; PLÜMER, L. *CityGML – Interoperable semantic 3D city models*. *ISPRS Journal of Photogrammetry and Remote Sensing*. 2012, **71**, 12–33.

[13] WANG, R; PEETHAMBARAN, J; DONG, C. *LiDAR Point Clouds to 3D Urban Models : A Review*. *Jstars*. 2018, **In Press**(January), 1–26.

[14] POPESCU, S C; WYNNE, R H. *Seeing the Trees in the Forest*. *Photogrammetric Engineering*

& Remote Sensing. 2004, **70**(5), 589–604.

[15] VULKAN, A; KLOOG, I; DORMAN, M; ERELL, E. *Modeling the potential for PV installation in residential buildings in dense urban areas*. *Energy and Buildings*. 2018, **169**, 97–109.

[16] MEEUS, J; H., J. *Astronomical algorithms*. B.m.: Willmann-Bell, 1991.

[17] GÁL, T; UNGER, J. *A new software tool for SVF calculations using building and tree-crown databases*. *Urban Climate*. 2014, **10**, 594–606.

[18] EC-JRC. *TMY Generator*. 2019 [accessed. 2019-01-08]. Available at: http://re.jrc.ec.europa.eu/pvgis5/tmy.html

[19] IGN. *Instituto Geográfico Nacional (España)*. 2019 [accessed. 2019-01-07]. Available at: http://www.ign.es

[20] PERONATO, G; REY, E; ANDERSEN, M. *3D model discretization in assessing urban solar potential: the effect of grid spacing on predicted solar irradiation*. *Solar Energy*. 2018, **176**, 334–349.